*Available online at* www.joac.info

ISSN: 2278-1862

Journal of Applicable Chemistry

2019, 8 (3): 1394-1403

(International Peer Reviewed Journal)

# Graphene Oxide-Manganese Oxide Composite (GO-$MnO_2$) As a Photocatalyst: A Comparative Study

**Meghavi Gupta[1]*, Neha Kapoor[1], Avinash Kumar Rai[1],**
**Rakshit Ameta[2] and Suresh C. Ameta[1]**

1. Department of Chemistry, PAHER University, Udaipur -313003, Rajasthan, INDIA
2. Department of Chemistry, J. R. N. Rajasthan Vidyapeeth (Deemed to be University) Udaipur-313001, Rajasthan, INDIA
Email: maggigupta03@gmail.com

**Accepted on 25th April, 2019**

---

## ABSTRACT

*A nanocomposite of graphene oxide (GO) and manganese dioxide ($MnO_2$) was prepared by mechanochemical method. Graphene oxide was synthesized by modified Hummer's method. As-formed nanocomposite was tested for its photoactivity by degrading trypan blue dye. It was found that the rate of photodegradation of trypan blue was faster with composite as compared to bare $MnO_2$ under optimum conditions. The optimum conditions for trypan blue degradation are: pH=6.5; trypan blue concentration=$1.5\times10^{-5}$ M; amount of composite=0.08 g; light intensity=50 mW $cm^{-2}$. The composite was also tested for its reusability.*

## Graphical Abstract

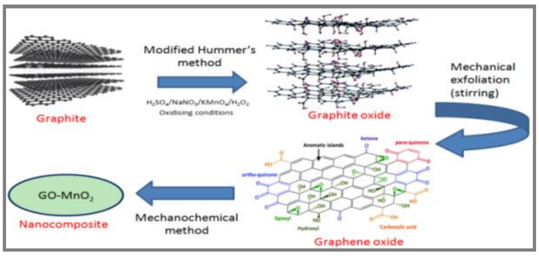

**Keywords:** Photocatalyst, Graphene Oxide-Manganese oxide, Wastewater, AOPs.

---

## INTRODUCTION

Wastewater discharge in water bodies like heavy metals and organic dyes has increased with rapid industrialization [1, 2]. Various methods to treat wastewater include photocatalysis [3], adsorption [4], advanced oxidation processes and so no catalytic treatment [5], etc.

Among these methods, advanced oxidation processes (AOPs) are low cost, efficient and environment friendly method to degrade different pollutants from water [6]. AOPs lead to the generation of hydroxyl radical ($^{\bullet}OH$), which is a very strong oxidizing agent and degrade the pollutant molecule into harmless smaller products.

Many of the GO-based materials nanocomposites are used in wastewater treatment for removal of dyes, heavy metals, insecticides and other carcinogenic chemicals. Due to the presence of large specific surface area and abundant functional groups in graphene oxide and reduced graphene oxide, they are considered better adsorbents.

$TiO_2$, ZnO, ZnS and $WO_3$ are most commonly used photocatalysts as they are reusable and have self-regenerated properties but the main drawback using these photocatalysts is that a high recombination of photogenerated electrons and holes is there. Since graphene oxide has superb mechanical strength, high catalytic activity, high surface area, excellent electron-transporting properties and low density, it is a superior photocatalyst than others and thus, a competent electron acceptor and can enhance photcatalytic activity of a semiconductor.

Chen *et al.,* [**7**] synthesized $Ag_3PO_4$/graphene-oxide ($Ag_3PO_4$/GO) composite by a liquid phase deposition method, and applied it for the photodegradation of methyl orange and rhodamine B in water under visible or UV-visible light. It was revealed that the $Ag_3PO_4$/GO composite with 15% GO content exhibited maximum activity under visible light. 86.7% methyl orange was degraded after a 50 min exposure of light while rhodamine B get 100% degraded within 30 min. It was suggested that holes played an important role in the direct oxidation of pollutants.

Graphene oxide-CdS composite was synthesized by Gao *et al.*, [**8**] via a two-phase mixing method. CdS nanoparticles were self-assembled on GO sheets at water/toluene interface. They studied photo degradation and photo disinfection activities of this composite (GO-CdS). They observed that this composite is highly efficient in photo degrading various water pollutants compared to pure CdS under visible light. Not only this, they also observed that the interactions between GO sheets and CdS nanoparticles prevent the photo-corrosion of CdS and percolation of $Cd^{+2}$.

$SnO_2$ nanoparticles are used as a photocatalyst for water purification but the recombination of the photogenerated electron and whole pairs limits its efficiency. Reddy *et al.,* [**9**] prepared tin oxide/graphene oxide ($SnO_2$/GO) nanocomposite to overcome this limitation. They investigated the photodegradation of methylene blue in aqueous heterogeneous suspensions and found an enhanced photoactivity as compared to bare $H_2O_2$. El-Hakam *et al.,* [**10**] synthesized a composite of graphene oxide with $TiO_2$ by a two step method. They hydrolysed titanium (IV) isopropoxide followed by hydrothermal method at 180°C. The resulting composites were calcined at different temperatures ranging from 300 to 550°C. Methylene blue was photo degraded using this composite and the rate of photodegradation for composite was found to be faster than pure $TiO_2$ under UV-Visible light. The reason for good performance of the composite can be attributed to uniform distribution of $TiO_2$ particles over graphene oxide sheets. A faster transfer of photogenerated electrons also resulted in controlling electron-hole pair recombination.

Hosseini and Babaei [**11**] compared the photocatalytic activity of graphene oxide/zinc oxde (GO/ZnO) nanocomposite with that of ZnO, GO and carbon nanotube/zinc oxide CNT/ZnO for the degradation of methylene blue from waste water. It was observed that methylene blue was 99% photodegraded over GO/ZnO surface under optimum conditions and it was far better than GO and CNT/ZnO surfaces.

Biswas and Oh [**12**] synthesized a photocatalyst $BiVO_4$-GO-PVDF (PVDF=polyvinylidene diflouride) by ultrasonication. The photocatalytic performance of the catalyst was examined by degrading methylene blue, rhodamine B and safranin-O in water under visible light. An enhanced photoactivity was observed in case of the composite as compared to that of pure $BiVO_4$ catalyst, $BiVO_4$ and PVDF decorated on the graphene sheet. This increased photoactivity may be attributed to effective transfer of photogenerated electron-hole pairs. They also conducted trapping experiments to identify the reactive species and observed that the direct whole oxidation reaction is dominant during photocatalytic reaction on the $BiVO_4$-GO-PVDF system.

Jeevitha *et al.,* [13] prepared tungsten oxide-graphene oxide ($WO_3$-GO) nanocomposite ultrasonically and used it as a photocatalyst, antibacterial and anticancer agent. They compared activity of the as-prepared composite with pure $WO_3$. Methylene blue (cationic) and indigo carmine (anionic) was photo degraded in presence of $WO_3$-GO nanocomposite and $WO_{3,}$ where enhanced photocatalytic efficiency was observed in case of composite. Exposure to light for 6 h resulted in improved inhibition for *Escherichia coli* and *Bacillus subtilis*. Anticancer activity of the nanocomposite $WO_3$-GO was tested against human lung cancer (A-549) cell line, where the IC50 value was observed to be 139.6 ± 4.53 µgmL$^{-1}$.

A very simple and high yielding room-temperature solid-state method was developed by Chen *et al.,* [14] to form graphene oxide-metal sulphide composites. They observed that the introduction of GO in metal sulphides resulted in an increased surface area. An enhancement in photoactivity was observed in degrading methyl orange under UV irradiation by the composite as compared to pure metal sulphides. This could be due to increased specific surface area and reduction in the recombination rate of electron-hole pairs.

A single step hydrothermal method was used to prepare molybdenum disulfide-graphene oxide ($MoS_2$-GO) composite hydrogel by Ding *et al.,* [15]. The photocatalytic activity of $MoS_2$-GO was investigated towards the degradation of methylene blue. They observed that photocatalytic activity of composite was higher in degrading methylene blue. The maximum rate of degradation of the dye was found to be 99% under solar light within 60 min. Graphene oxide and $MnO_2$ (GO-$MnO_2$) composite was synthesized by Saroyan *et al.,* [16] and used for photodegradation of an azo dye, reactive black 5. They observed that GO-$MnO_2$ nanocomposite degrades the RB5 dye at a much faster rate as compared to pure $MnO_2$.

El-Shafai *et al.,* [17] synthesized graphene oxide and allowed it to react with $Fe_3O_4$ and $ZrO_{2.}$ This reaction leads to the formation of two different nanocomposites namely graphene oxide-iron oxide (GO-$Fe_3O_4$) and graphene oxide-iron oxide-zirconium oxide (GO-$Fe_3O_4$@$ZrO_2$). Introduction of $Fe_3O_4$ and $ZrO_2$ in GO resulted in thinning of band gap of GO making the composite better photocatalyst and adsorbent. Rhodamine B dye was selected as a model pollutant. The antibacterial activity of GO and GO-metal oxide was also examined against gram-negative and gram-positive bacteria.

A composite constituting of three dimensional GO (3D-GO), polyvinyl alcohol (PVA), and $TiO_2$microspheres (3D-GO/PVA/$TiO_2$) was fabricated by Wang *et al.,* [18] via a one-pot synthesis using aqueous suspension of PVA and 3D-GO sheets in presence of $TiO_2$ microspheres. The excellent performance of the catalyst 3D-GO/PVA/$TiO_2$ may be due to enhanced adsorption performance by the rich p-conjugation structure of GO and 3D-GO/PVA sheets. The adsorption of methylene blue and methyl violet onto the composite was observed in dark for 30 min and then it is exposed to solar light for 2 h. Methylene blue and methyl violet were degraded 95% and 96%, respectively. They also showed that this composite is stable and reusable.

## MATERIALS AND METHODS

**Preparation of graphene oxide (GO):** Three different conventional methods namely Hummer's [19], modified Hummer's [19] and Tour's method [20] are available for preparation of graphene oxide. It was observed that composite of GO with $MnO_2$ gave excellent results, when graphene oxide synthesised by modified Hummer's method was used for preparation of composite and dye degradation. So, further photocatalytic studies were conducted using graphene oxide synthesized by modified Hummer's method forming a composite with $MnO_2$.

**Preparation of composites:** The two components of the composite i.e. GO and $MnO_2$ were homogeneously ground using agate mortar and pestle (mechanochemical method). The composites were prepared in three different ratios (1:1, 1:2 and 2:1 of GO-$MnO_2$) and their photoactivity was compared. Composite with 2:1 ratio (GO-$MnO_2$) gave superior results in comparison to composites with 1:1 and 1:2 ratios for the degradation of trypan blue. Therefore, further experiments were carried out with composite of GO-$MnO_2$ in the ratio of 2:1.

**Characterization of composite:** The EDX results confirmed the presence of different elements present in composite of GO with $MnO_2$. The results are tabulated in table 1.

**Table 1**. EDX Data

| Elements | Atomic % (GO-$MnO_2$) |
|---|---|
| **C** | 42.23 |
| **Mn** | 20.88 |
| **O** | 36.89 |

FTIR (Fourier Transform Infrared) spectrum was recorded using F.T. Infra-Red Spectrophotometer Model RZX(Perkin Elmer)to determine the different functional groups present in the composite (GO-$MnO_2$). The FTIR spectrum of GO-$MnO_2$ is represented in figure 1.

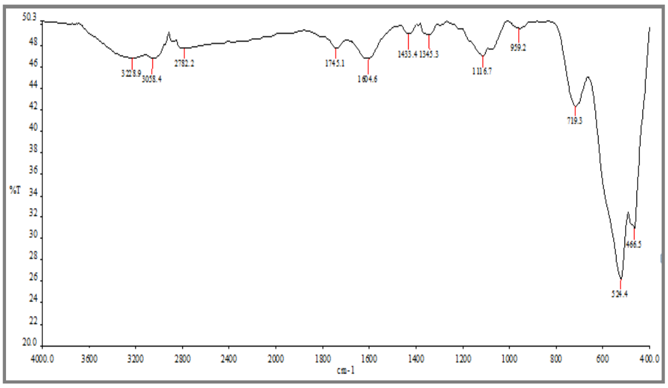

**Figure 1.** FTIR spectrum of GO-$MnO_2$ nanocomposite.

The IR spectrum of GO has been reported elsewhere, which confirmed the GO was formed [21]. In case of the composite (GO-$MnO_2$), a broad peak at 3228.9 $cm^{-1}$ represents O-H stretching vibrations of the C-OH groups and water molecule. Peaks at 524 and 446 $cm^{-1}$ (around ~500 $cm^{-1}$) represents Mn-O bond vibrations present in the composite (GO-$MnO_2$) [11].

Using X-ray Diffractometer Panalytical.s X.Pert Pro., X-ray diffraction patterns were recorded for the naocomposite (GO-$MnO_2$). The X-ray pattern of the composite is shown in figure 2. Using Debye-Scherrer equation, the average particle size for the composite (GO-$MnO_2$) was calculated to be 19.09 nm.

**Photocatalytic degradation of trypan blue:** The dye trypan blue was allowed to degrade under visible light in order to study photocatalytic activity of the composite (GO-$MnO_2$). The light source was a 200 W tungsten Phillips lamp. A stock solution of the dye ($1.0 \times 10^{-3}$ M) was prepared by dissolving 0.0960 g of dye in 100 mL of doubly distilled water. Using this stock solution, working solutions of various concentrations were prepared by dilution. The pH of the samples was measured using a digital pH meter (Systronics model 335) and the pH was adjusted by addition of standard solution of 0.1 N sodium hydroxide and 0.1 N sulphuric acids. The wavelength of maximum absorption for trypan blue was found to be at 610 nm. Solarimeter (Suryamapi CEL 201) was used to measure the light intensity for the experiments. The absorbance (A) of the dye is observed using a spectrophotometer (Systronics model 106). A petridish filled with water was used as a filter to cut off thermal radiations.

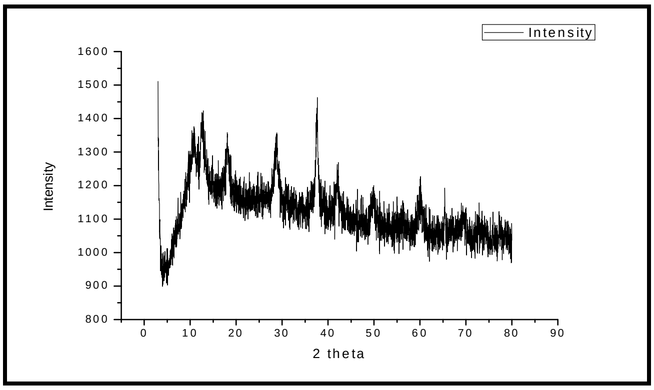

**Figure 2.** XRD of GO-$MnO_2$.

**Control experiments:** Dye solution, of a particular concentration, was equally distributed in four different beakers.

- The first beaker having dye solution was placed in dark.
- The second beaker with dye solution was exposed to light.
- The third beaker containing dye solution with the composite (GO-$MnO_2$) was placed in dark.
- The fourth beaker containing dye solution and composite (GO-$MnO_2$) was irradiated with light.

After 4 h, the degradation was observed only in beaker, where both; composite (GO-$MnO_2$) and light were present. It is clear that the presence of light and photocatalyst (GO-$MnO_2$) was necessary for the degradation of the dye.

It was found that the absorbance of the dye solution decreases with time. The rate of degradation of trypan blue followed pseudo-first order kinetics and the rate constant could be calculated from the slope of the plot between log A vs time using the formula.

$$k = 2.303 \times \text{slope}$$

## RESULTS AND DISCUSSION

**Typical runs:** The typical runs for the system GO-$MnO_2$ with the dye trypan blue is tabulated in the table 2 and graphically represented in figure 3.

**Table 2.** Typical Runs

| Time (min) | GO-$MnO_2$ (nanocomposite) | | $MnO_2$ | |
|---|---|---|---|---|
| | A | 1 + log A | A | 1 + log A |
| 0 | 0.626 | 0.7965 | 0.652 | 0.8142 |
| 10 | 0.543 | 0.7348 | 0.624 | 0.7952 |
| 20 | 0.466 | 0.6684 | 0.591 | 0.7716 |
| 30 | 0.398 | 0.5999 | 0.565 | 0.7520 |
| 40 | 0.344 | 0.5366 | 0.537 | 0.7299 |
| 50 | 0.292 | 0.4654 | 0.510 | 0.7076 |
| 60 | 0.251 | 0.3998 | 0.487 | 0.6875 |
| 70 | 0.216 | 0.3344 | 0.463 | 0.6656 |
| 80 | 0.185 | 0.2672 | 0.442 | 0.6454 |
| 90 | 0.158 | 0.1986 | 0.422 | 0.6253 |
| 100 | 0.135 | 0.1303 | 0.401 | 0.6031 |

k (GO-$MnO_2$) = $2.55 \times 10^{-4}$ $sec^{-1}$, k ($MnO_2$) = $8.31 \times 10^{-5}$ $sec^{-1}$

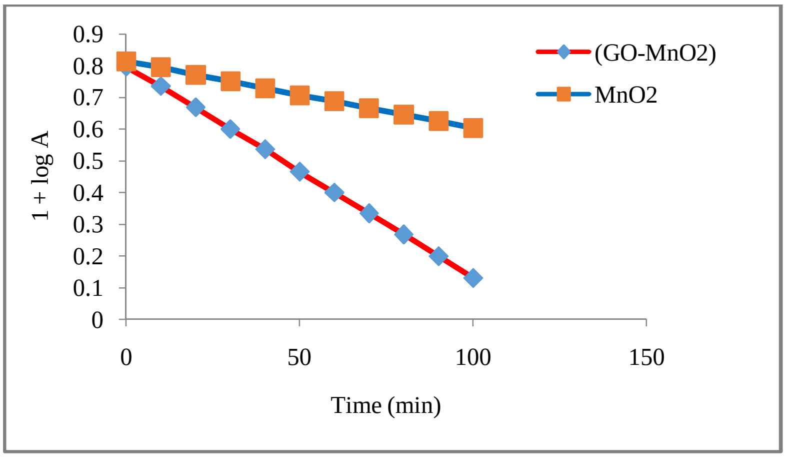

**Figure 3.** Typical runs.

### Influence of various parameters on the rate of degradation:

**Effect of pH:** pH is one of the most prominent factors that is likely to influence the rate of degradation of trypan blue. So, pH was varied from 4.0 to 9.5. It was observed that as the pH was increased, rate of dye degradation also increases to an optimum pH (6.5) and then there was a fall (Figure 4).

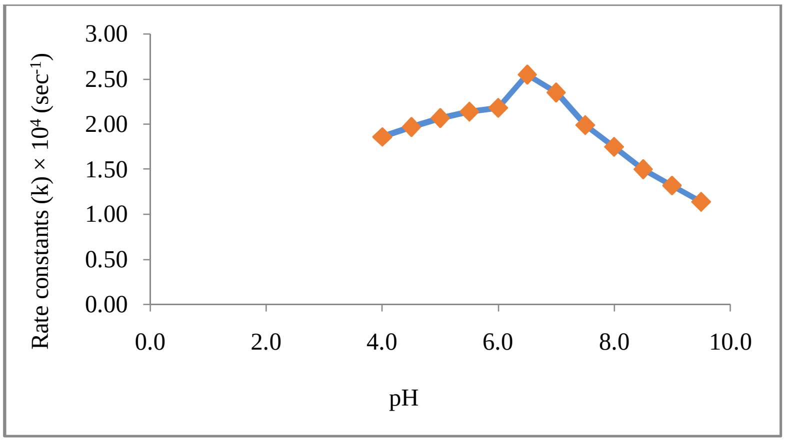

**Figure 4.** Effect of pH.

As the pH was decreased, the dye will be converted to its almost neutral or neutral form. This form of the dye will face no attraction/repulsion with the positively charged surface of the composite because of adsorbed protons. As a consequence, rate of degradation decreases on decreasing pH (increasing acidity). On the other hand, the dye will remain in its anionic form in the basic range. As the pH was increased above 6.5, trypan blue (in its anionic form) will face a force of repulsion with the negatively charged surface of the composite due to adsorption of $OH^-$ ions; thus, resulting in a decrease in the rate of degradation.

**Effect of dye concentration:** The concentration of trypan blue was varied from $0.5 \times 10^{-5}$ to $4.5 \times 10^{-5}$ M to observe the effect of dye concentration on the rate of degradation of dye in the presence of the photocatalyst (GO-$MnO_2$). A regular increase in the rate constant was observed till the optimum dye concentration of $1.5 \times 10^{-5}$ M was reached and there onwards, the rate decreases on increasing the concentration of dye further (Figure 5). This may be due to increased number of dye molecules available for excitation and energy transfer but after the optimum concentration, the rate falls, which may be possibly because of the fact that the dye will behave as a filter and it will not allow the sufficient light to reach to the surface of the composite. Thus, the effective light intensity reaching the surface of the photocatalyst decreases, and so is the rate.

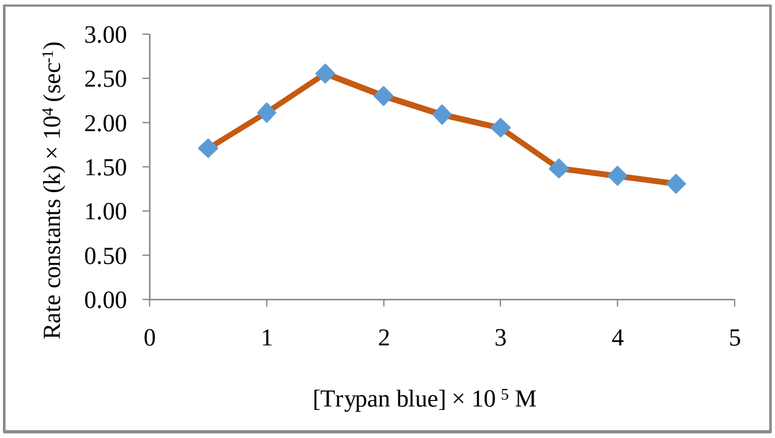

**Figure 5.** Effect of dye concentration.

**Effect of amount of catalyst:** Amount of catalyst was varied from 0.01 to 0.10 g (Figure 6). An increase in rate of degradation of trypan blue was observed with an increase in amount of catalyst due to increase in exposed surface area, but only to an optimum amount (0.08 g). Further increase in amount will only result in formation of multilayers, which leads to the recombination of the generated electron-hole pairs and thus, a fall in rate was observed.

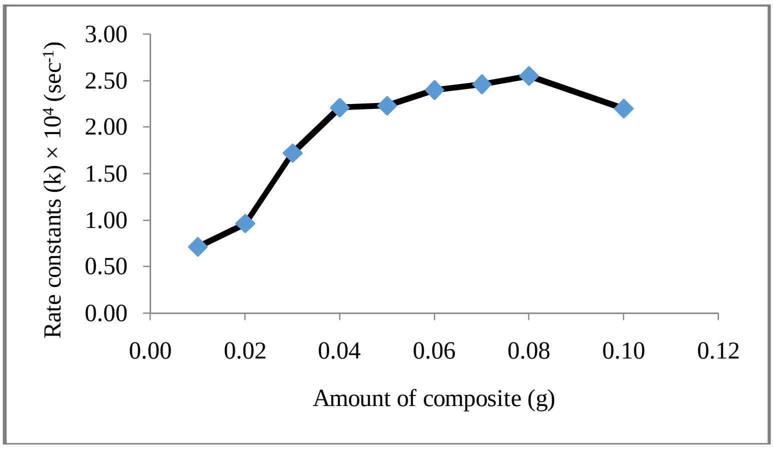

**Figure 6.** Effect of amount of composite.

**Effect of light intensity:** The effect of light intensity was monitored by varying the distance between the light source and the exposed surface area. The light intensity was varied in the range 20.0 to 70.0 mWcm$^{-2}$ (Figure 7). The results showed that a regular increase in rate was observed till 50.0mWcm$^{-2}$. This may be due to increased number of photons striking the surface of the composite (photocatalyst) per unit area and per unit time. Then a fall in rate may be due to some thermal side reactions.

**Mechanism:** To determine the active oxidant species, a quenching test was conducted. It was observed that the rate of degradation of trypan blue falls significantly on using isopropyl alcohol (a hydroxyl radical scavanger). Thus, it may be concluded that the active oxidizing species was $^{\bullet}OH$ (hydroxyl radical).

Mechanism of degradation of trypan blue has been proposed as:

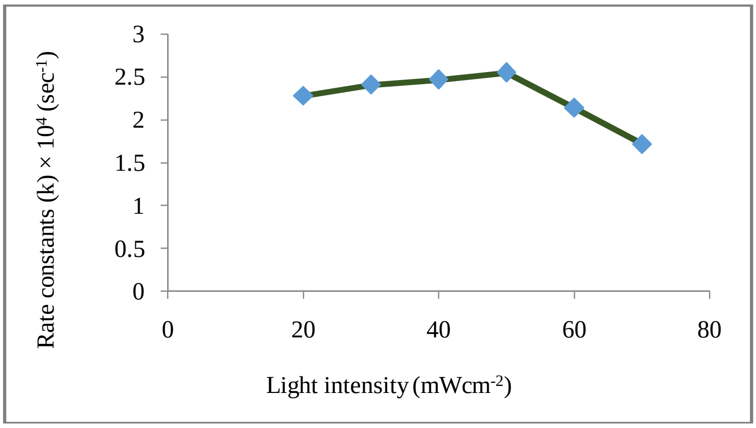

**Figure 7.** Effect of light intensity.

$$^{1}\mathrm{TB}_0 \xrightarrow{h\nu} {}^{1}\mathrm{TB}_1 \qquad \ldots (1)$$

$$^{1}\mathrm{TB}_1 \xrightarrow{\mathrm{ISC}} {}^{3}\mathrm{TB}_1 \qquad \ldots (2)$$

$$\mathrm{SC} \xrightarrow{h\nu} \mathrm{SC}\ [h^{+}(\mathrm{VB}) + e^{-}(\mathrm{CB})] \qquad \ldots (3)$$

$$h^{+} + \mathrm{OH}^{-} \longrightarrow {}^{\bullet}\mathrm{OH} \qquad \ldots (4)$$

$$^{3}\mathrm{TB}_1 + {}^{\bullet}\mathrm{OH} \longrightarrow \text{Leuco TB} \qquad \ldots (5)$$

$$\text{Leuco TB} \longrightarrow \text{Products} \qquad \ldots (6)$$

Here, TB is Trypan blue.

Trypan blue absorbs light radiations of a suitable wavelength and get converted to its excited singlet state. This excited singlet state of the dye undergoes inter system crossing (ISC) and changes to its triplet state. Meanwhile, the semiconducting photocatalyst (GO-$MnO_2$ nanocomposite) also absorbs light energy and the electron in the valence band get excited to the conduction band, which results in hole generation in the valence band. This hole will withdraw an electron from the hydroxyl ion ($OH^{-}$) to form hydroxyl radical ($^{\bullet}OH$). These $^{\bullet}OH$ radical will now behave as the reactive oxidizing species, which oxidizes trypan blue to its leuco form and finally leuco form of the dye degrades to smaller non-toxic products.

## APPLICATION

Various applications of graphene oxide and its composite are found in Sensors, Biosensors, Electronic devices, Antibacterial activity, Biomedical, optical applications, Photocatalyst [22-24] and Energy storage devices.

## CONCLUSION

- Modified Hummer's method (for the synthesis of GO) has been reported to be the best method for degradation of trypan blue with composite of GO with $MnO_2$.
- The composite of GO with $MnO_2$ is best, when used in the ratio 2:1 (GO: $MnO_2$).
- The reactive oxidant species was found to be $^{\bullet}OH$ (hydroxyl radical) on the basis of the scavenger test.
- The composite can be reused 4 times with no or very little loss in its photoactivity.

## REFERENCES

[1]. N. Hashim, Z. Muda, M. Z. Hussein, I. M. Isa, A.Mohamed, A. Kamari, A brief review on recent graphene oxide-based material nanocomposites: Synthesis and applications, *J. Mater. Environ. Sc*i., **2016**, 7(9), 3225-3243.

[2]. J. Liu, G. Liu, W. Liu,Preparation of water-soluble β-cyclodextrin/poly(acrylic acid)/graphene oxide nanocomposites as new adsorbents to remove cationic dyes from aqueous solutions, *Chem. Eng. J.*, **2014**, 257, 299-308.

[3]. V. K. Gupta, T. Eren, N. Atar, M. L. Yola, C. Parlak, H. Karimi-Maleh,$CoFe_2O_4@TiO_2$ decorated reduced graphene oxide nanocomposite for photocatalytic degradation of chlorpyrifos, *J. Mol. Liq.*, **2015**, 208,122-129.

[4]. P. K. Boruah, D. J. Borah, J. Handique, P. Sharma, P. Sengupta, M. R. Das, Facile synthesis and characterization of $Fe_3O_4$ nanopowder and $Fe_3O_4$/ reduced graphene oxide nanocomposite for methyl blue adsorption: A comparative study, *J. Environ. Chem. Eng.*, **2015**, doi:10.1016/j.jece.2015.06.030.

[5]. S. Thangavel, N. Raghavan, G. Kadarkarai, S.-J. Kim, G. Venugopal, Graphene-oxide (GO)–$Fe^{3+}$ hybrid nanosheets with effective sonocatalytic degradation of reactive red 120 and study of their kinetics mechanism, *Ultrason Sonochem*., **2015**, 24, 123-131.

[6]. S. Kumar, C. Terashima, A. Fujishima, V. Krishnan, S. Pitchaimuthu in M. Naushad (Ed.), A New Generation Material Graphene: Applications in Water Technology, *Springer Nature, Basingstoke*, **2019.**

[7]. G. Chen, M. Sun,Q. Wei, Y. Zhang, B. Zhu, B. Du, $Ag_3PO_4Ag_3PO_4$/graphene-oxide composite with remarkably enhanced visible-light-driven photocatalytic activity toward dyes in water, *J. Hazard. Mater.*, **2013**, 244–245, 86–93.

[8]. P. Gao, J. Liu, D. D. Sun, W. Ng, Graphene oxide–CdS composite with high photocatalytic degradation and disinfection activities under visible light irradiation, *J. Hazard. Mater*., **2013**, 250–251, 412-420.

[9]. P. R. Reddy, V. Shireesha, V. Malapat, K. V. Rao, Y. Aparna,Degradation of methylene blue from water under sunlight using $SnO_2$/graphene oxide composite, *Int. J. Eng. Adv. Technol*., **2015**, 4 (6), 2249-8958.

[10]. S.A. El-Hakam, A. I. Ahmed, S.M. El-dafrawy, A.A. Ibrahim, M.S. Adly, Application of nanostructured graphene oxide/titanium dioxide composites for photocatalytic degradation of methylene blue dye under UV-visible light, *Int. J. Modern Chem*., **2016**, 8(1), 27-37.

[11]. S. A. Hosseini, S. Babaei, graphene oxide/zinc oxide (GO/ZnO) nanocomposite as a superior photocatalyst for degradation of methylene blue (MB)-process modeling by response surface methodology (RSM), *J. Braz. Chem. Soc.*, **2017**, 28 (2), 299-307.

[12]. M. R. U. D. Biswas, W.-C. Oh , Synthesis of $BiVO_4$-GO-PVDF nanocomposite: An excellent, newly designed material for high photocatalytic activity towards organic dye degradation by tuning band gap energies, *Solid State Sci.*, **2018**, 80, 22-30.

[13]. G. Jeevitha, R. Abhinayaa, D. Mangalaraj, N. Ponpandian , Tungsten oxide-graphene oxide ($WO_3$-GO) nanocomposite as an efficient photocatalyst, antibacterial and anticancer agent, *J. Phys. Chem. Solids*, **2018**, 116, 137–147.

[14]. F.-J. Chen, Y.-L. Cao, D.-Z. Jia, A room-temperature solid-state route for the synthesis of graphene oxide–metal sulfide composites with excellent photocatalytic activity, *Cryst. Eng. Comm.*, 2013, 15, 4747-4754.

[15]. Y. Ding, Y. Zhou, W. Nie, P. Chen, $MoS_2$–GO nanocomposites synthesized via a hydrothermal hydrogel method for solar light photocatalytic degradation of methylene blue, *Appl. Surf. Sci.*, **2015**, 357, 1606–1612.

[16]. H. Saroyan, G. Z. Kyzas, E. A. Deliyanni, Effective dye degradation by graphene oxide supported manganese oxide, *Processes*, **2019**, 7, doi:10.3390/pr7010040.

[17]. N. M. El-Shafai, M. E. El-Khouly, M. El-Kemary, M. S. Ramadana, M. S. Masoud, Graphene oxide–metal oxide nanocomposites: Fabrication, characterization and removal of cationic rhodamine B dye, *RSC Adv.*, **2018**, 8, 13323-13332.

[18]. M. Wang, L. Cai, Q. Jin, H. Zhang, S. Fang, X. Qu et al., One-pot composite synthesis of three-dimensional graphene oxide/poly (vinyl alcohol)/$TiO_2$ microspheres for organic dye removal, *Sep. Purif. Technol.*, **2017**, 172, 217–226.

[19]. B. Paulchamy , G. Arthi, B. D. Lignesh, A simple approach to stepwise synthesis of graphene oxide nanomaterial, *J. Nanomed. Nanotechnol*., **2015**, 6(1), doi: 10.4172/2157-7439.1000253.

[20]. D. C. Marcano, D. V. Kosynkin, J. M. Berlin, A. Sinitskii, Z. Sun, A. Slesarev, L. B. Alemany, W. Lu, J. M. Tour, Improved synthesis of graphene oxide, *Acs Nano*, **2010**, 4 (8), 4806-4814.

[21]. M. Gupta, J. Bhatt, Ruchi, R. Ameta, S. C. Ameta, Use of graphene oxide-zinc oxide composite in photocatalytic degradation of victoria blue b, *J. Nanosci. Technol*., **2019**, In Press.

[22]. S. S. Ryali, P. D. Sanasi, Effect of graphene oxide on nano titania particles in visible light induced photocatalytic degradation of Congo red, *J. Applicable Chem*., **2017**, 6(6), 1200-120.

[23]. C. Pragathiswaran, B. M. Abbubakkar , P. Govindhan, K. A. S. Abuthahir, Synthesis of $TiO_2$ and ZnO nano composites with graphene oxide photocatalytic reduction and removal of chromium (VI) in aqueous solution, *J. Applicable Chem*., **2015**, 4(2), 525-532.

[24]. Ruchi, A. K. Rai, J. Bhatt, R. Ameta,S. C. Ameta, Photocatalytic degradation of azure B by reduced graphene oxide-copper sulphide composite (rGO-CuS): A green approach towards environmental remediation, *J. Applicable Chem*., **2019**, 8 (2),794-800.